STM JOURNALS

Journal of
Polymer & Composites

https://journals.stmjournals.com/jopc

ISSN: 2321-2810 (Online)
ISSN: 2321-8525 (Print)
Volume 14, Issue 5, 2026
September–October
DOI (Journal): 10.37591/JoPC

Research JoPC

Ultrasonic Dispersion of Halloysite Nanotubes for Enhanced Mechanical, Thermal, and Morphological Performance of Epoxy Composites

Ritesh Dixit[1], Anil Kumar[2], Shakun Srivastava[3], Ashwani Sharma[4], Kheelraj Pandey[4,*]

Abstract

Halloysite nanotube (HNT)-reinforced epoxy nanocomposites were prepared by mixing HNT with bisphenol-A epoxy (LY 556) using ultrasonication, followed by compression molding. HNT contents of 0–5 wt.% were used. The composites were evaluated for tensile strength, flexural strength, Shore D hardness, Izod impact strength, and thermal stability using thermogravimetric analysis (TGA). The fractured tensile surfaces were also examined to understand the failure mechanism and interaction between HNT and the epoxy matrix. Among all compositions, the composite containing 3 wt.% HNT showed the best overall performance. Compared with the neat epoxy, it achieved improvements of 110.5% in Izod impact strength, 55.4% in ultimate tensile strength, 34.8% in flexural strength, and 30.7% in thermal stability. The addition of HNT also improved the Shore D hardness of the epoxy composites. However, higher HNT contents reduced the performance due to particle agglomeration and poor dispersion. Although several studies have investigated HNT/epoxy composites, limited attention has been given to achieving uniform HNT dispersion and establishing a clear relationship between dispersion quality, processing conditions, and mechanical and thermal properties. The effect of ultrasonication on filler dispersion, viscosity, and processability has also not been studied sufficiently. The present study addresses these gaps by using an ultrasonication-assisted dispersion method to achieve better HNT distribution in the epoxy matrix. The mechanical, thermal, and morphological properties were studied systematically. The results establish a clear relationship between HNT dispersion, interfacial bonding, and composite performance. The study identifies 3 wt.% HNT as the optimum filler content, while higher contents lead to agglomeration and reduced properties. Overall, the work provides a useful understanding of the relationship between processing, microstructure, and performance of HNT/epoxy nanocomposites.

Keywords: Epoxy, halloysite nanotube (HNT), tensile, thermal stability, microstructure

***Author for Correspondence**
Kheelraj Pandey
E-mail: kpandey1@lko.amity.edu

[1]Ph.D. Scholar, Department of Mechanical Engineering, Amity University, Lucknow, Uttar Pradesh, India
[2]Professor, Department of Mechanical Engineering, Amity University, Lucknow, Uttar Pradesh, India
[3]Associate Professor, Department of Mechanical Engineering, Pranveer Singh Institute of Technology, Kanpur, Uttar Pradesh, India
[4]Assistant Professor, Department of Mechanical Engineering, Amity University, Lucknow, Uttar Pradesh, India

Received Date: July 30, 2026
Accepted Date: August 14, 2026
Published Date: August 17, 2026

Citation: Ritesh Dixit, Anil Kumar, Shakun Srivastava, Ashwani Sharma, Kheelraj Pandey. Ultrasonic Dispersion of Halloysite Nanotubes for Enhanced Mechanical, Thermal, and Morphological Performance of Epoxy Composites. Journal of Polymer & Composites. 2026; 14(5): 212–226p.

INTRODUCTION

Polymer based composite components in transportation, biomedical applications and other several utilities are in attraction in the interest of researchers due to light weight, sufficient strength and designability [1–5]. Whereas in these composites, the presence of dispersed nanotube particles provides a potential to increase in mechanical properties and thermal stability, which are in great demand due to a wide range of fulfillment for above applications [6]. From literature, it has been drawn that several types of filler materials – like carbon nanotubes [7, 8], silicate clays [9], Nano silica [10], and graphene [11] – are the key reinforcement particles with a consolidated effect, provide an enhancement of

mechanical characteristics and thermal properties for fabricated epoxy polymer composites. Subsequently, the changes provide flexibility and durability of the components with a reduction in the cost [12]. Carbon nanotube-based polymer composite increases the mechanical properties which are adopted; however, it conjointly provides a hazardous effect on the environment [13].

Moreover, halloysite nanotube ($Al_2Si_2O_5(OH)_4.2H_2O$, clay mineral) is a naturally available material, which depicts similar effects on the properties of the polymer-based composites. Accordingly, halloysite nanotubes (HNTs) are more suitable nanofiller material due to size, distribution within the layer of the composite and excellent level of aspect ratio for dispersion and distribution [14]. It has the capability as an agent for nanocontainer/nanofiller among varied applications for better mechanical and thermal properties and morphological refinement. Further use of nanotubular halloysite particulate as a filler in polymer composite has been interesting due to good dispersible property and positioning effect of SiO_2 tetrahedra on the composed interfacial surfaces of the HNT's. It has relative tubular morphology, unique crystal structure, and relative flexibility with unusual charge distribution on the inner wall of the tubes [15, 16]. However, HNT's are one amongst the foremost appropriate reinforcements/carriers for the polymer-based composite with satisfactory improvement on the HNT's based polymer composite. Halloysite nanotubes are easily available and are cost effective than other different nanotubes such as CNT's [9, 17].

Hemp waste (herds/shives, waste fibers, matting) as a substrate for mycelium-grown biocomposites: a brief bibliography. It proposes "myco-composites" – like Trametes versicolor and Pleurotus ostreatus – to replace polystyrene foam by comparing compression strength, water absorption, and biodegradability [18]. Experimental investigation on polyester composites with snake grass fiber reinforced with Sal wood and Babool sawdust fillers. The S4 formulation got the best balance: 56 MPa tensile, 85 MPa flexural, 6.98 J impact, 84 Shore D hardness and the lowest water absorption of 21%. The SEM and FTIR indicated superior interfacial bonding at optimum ratios of filler-fiber [19].

Study the effect of fiber loading on mechanical, morphological and dynamic mechanical behavior of Calamus tenuis fiber reinforced epoxy composites [20]. First report on the usage of Aristida hystrix fibers mixed in polyester at 0 to 9 wt% and ball-milled to nano size. The highest performance was obtained at 5 wt% (30.13 MPa tensile, 43.685 MPa flexural, 1.87 kJ/m² impact) and after this level, agglomeration and increased moisture absorption occurred [21]. An overview of the incorporation of IoT sensors into polymer composites for real-time monitoring of temperature, strain, humidity and environmental exposure. Data transmission, cloud analytics, digital twins and problems on standardization, data security and interoperability. It also contains a good critical piece on overestimation of IoT advantages in the "echo-chamber" [22]. Examine the impact of stacking sequence on hybrid woven fiber metal laminates of jute, banana and basalt textiles with aluminum diamond micro-expanded mesh in epoxy. The five layers sequence BBnABnB showed the greatest performance in compressive strength (25.7 MPa), ILSS (25.2 MPa) and Izod impact (2.98 J) [23].

This study aims to fabricate epoxy/HNT nano-composites and evaluate the consequences of nanotubular halloysite (HNT) on thermal stability along with the mechanical performance at different filler loadings. Epoxy/HNT nanocomposites containing 1–5 wt.% HNT were prepared and characterized to assess the influence of HNT on tensile, impact, hardness, and flexural properties. Microstructural analysis showed a gradual increase in composite density with increasing HNT content, suggesting better filler dispersion with stronger interfacial interaction among the HNT and epoxy matrix. These improvements demonstrate the effectiveness of HNT as a reinforcing filler for enhancing the overall performance of epoxy nanocomposites.

EXPERIMENTAL

Materials

Commercially available medium-viscosity DGEBA epoxy resin, LY 556 (diglycidyl ether, i.e., bisphenol-A), having specific gravity of 1.16, was utilized as the matrix material. TETA hardener, HY 951 (triethylenetetramine), with a specific gravity of 0.95, served as the curing agent. Both materials were procured from Ciba Geigy Ltd., Mumbai, India, and used to fabricate the epoxy/HNT nanocomposites.

Epoxy resin and hardener was used in liquid form in a specific ratio by wt. % (10:1); whereas Halloysite nanotube is uniformly mixed in varying proportions for fabrication of composite sheet. The Halloysite nanotube was used as reinforcement in epoxy (supplied by Sigma Aldrich, USA) and purity of HNT's is more than 98%.

Nanocomposite Preparation

HNT/x epoxy polymer nanocomposites (x = 1 to 5 wt. %) were fabricated by casting method and mixed under an ultrasonicated environment. During ultrasonication, the epoxy and reinforcement mixture was treated with ultrasonic waves at 50% amplitude for 1 h using a "Rivotek sonicator" (Model XT 546, 700 W), shown in Figure 1(a).

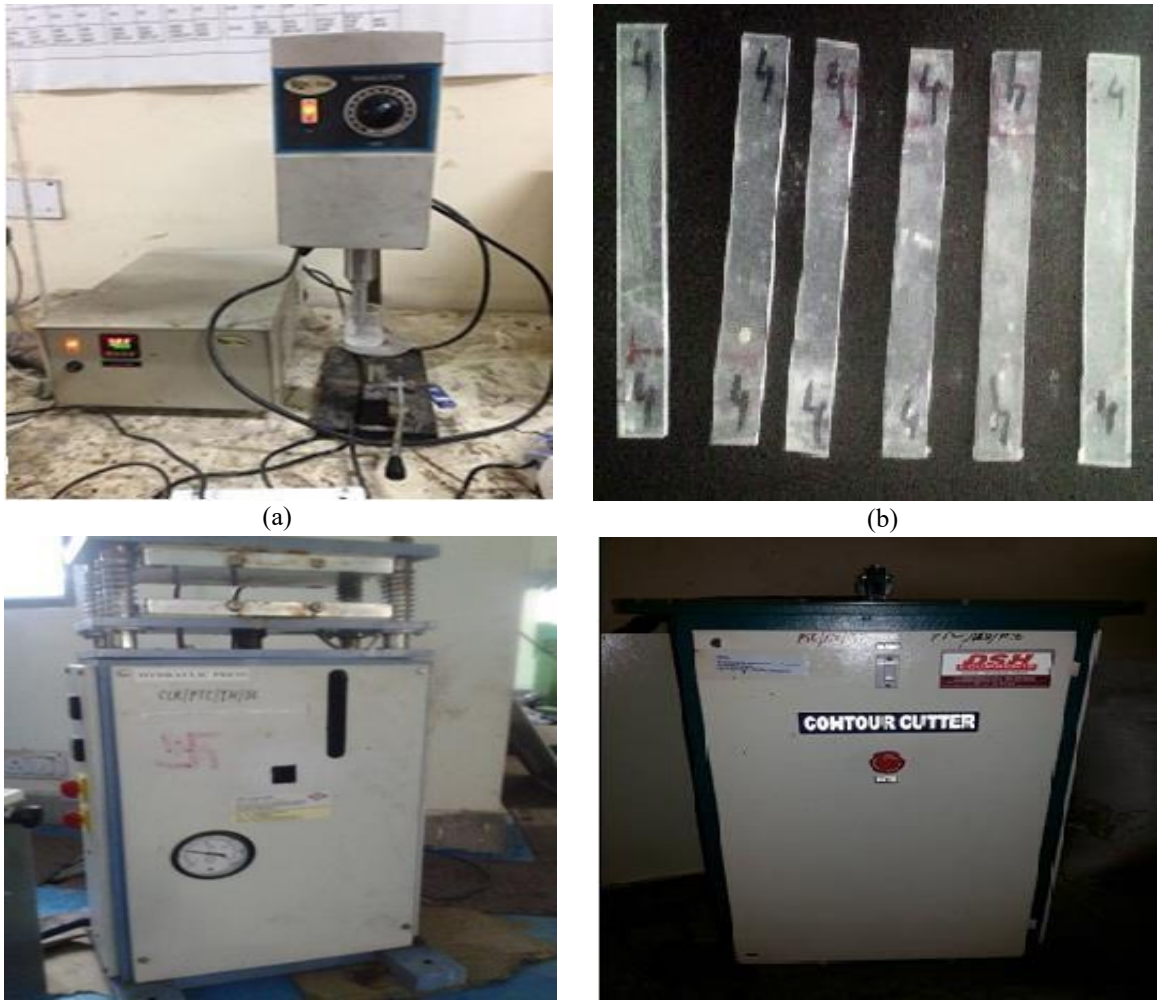

(a) (b) (c) (d)

Figure 1. (a) ultrasonication during the mixing, (b) fabricated composite sheet, (c) compression of the HNT/epoxy mixture, and (d) contour cutting apparatus for composite sheet.

The composite mixture temperature increases slowly during the sonication process and reaches up to 80^0. After ultrasonication, it was noticed that mixture is apparent in thin form which indicates that viscosity reduces. This reduction in viscosity was a basic need for further fabrication of specimens. The epoxy and halloysite mixture were degassed for 30 minutes after the addition of a triethylenetetramine curing agent (10 wt.%) and then filled in the stainless steel (150 * 150 * 3 mm) mold. Triethylenetetramine cured samples (shown in Figure 1(b)) were hydraulically compressed in an apparatus, have been cured at temperature environment of room environment for 24 h (shown in Figure 1(c)). Contour cutting machine, shown in Figure 1(d), was used to cut composite sheets in shapes according to ASTM for various testing.

TESTING AND CHARACTERIZATION

Properties with Mechanical Attributions

The properties mechanical in nature of the fabricated HNT/epoxy nanocomposites, with ultimate tensile strength, Young's modulus, elongation at break, and flexural strength, was investigated with Universal Testing Machine (UTM, Instron 3382) at room temperature (18–25°C), as shown in Figure 2(a).

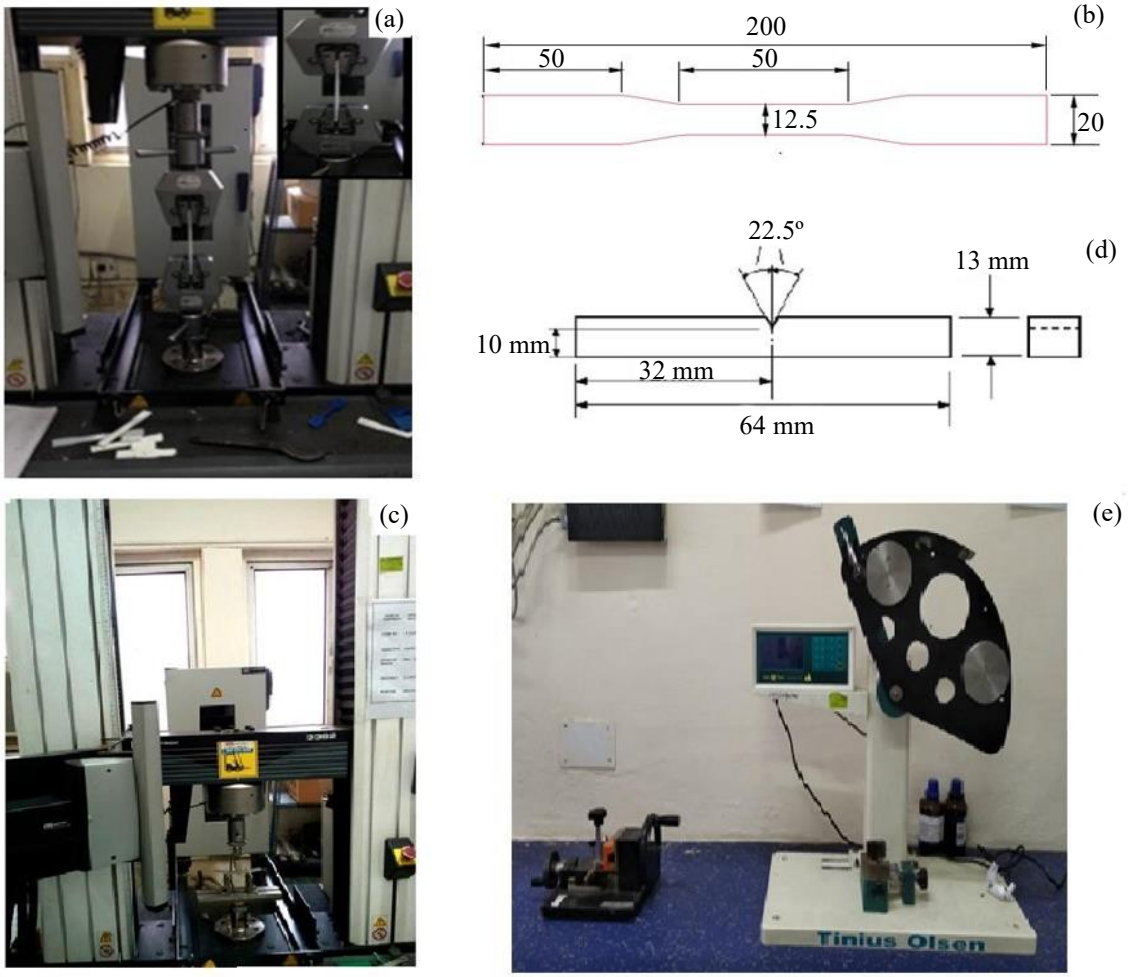

Figure 2. (a) Tensile testing of the samples, (b) ASTM standard for tensile testing, (c) flexural testing of samples, (d) ASTM standard for tensile testing, and (e) impact testing of the samples.

Tensile specimens with a gauge-length, i.e., 50 mm was prepared according to ASTM D638 standards (Figure 2(b)) and tested using an extensometer with crosshead speed of 0.3 mm/s.

Flexural testing was carried out according to ASTM D790 using the same UTM under a 3-point bend shape (Procedure A) with support distance of 48 mm, as highlighted in Figure 2(c). Izod impact strength of the nanocomposites was estimated according to ASTM D256 (Method A) using an Izod impact testing apparatus (Tinius Olsen) at room temperature, as highlighted in Figure 2(d) and (e).

Hardness of fabricated composites was measured using a Shore D durometer according to ASTM D2240 standards at room temperature. For reliable and repeatable measurements, five readings were taken for each specimen, and the three most consistent values were used for further analysis.

Thermo-Gravimetric Analysis (TGA)

The thermal steadiness and decomposition characteristics of fabricated nanocomposites were

evaluated using a thermos-gravimetric analyzer (TGA, Perkin–Elmer Pyris). Measurements were carried out between 50–720°C with rate of heating at 10°C/min in an atmosphere of nitrogen maintain a flow rate of 20 mL/min. For every composite sample, at least two samples were tested under the same environment.

Morphological Study

The microstructural features of fractured surfaces of tensile composite samples were examined with a scanning electron microscope (SEM, JEOL JSM-6610, JEOL, NY). Before SEM analysis, the fractured surfaces were treated with a thin gold film using a sputtering unit to enhance electrical conductivity and obtain clear SEM images. The coated specimens were subsequently placed in the SEM chamber for detailed microstructural observation.

RESULTS AND DISCUSSION

Mechanical Properties

Obtained results of fabricated nanocomposite for mechanical properties are summarized in Table 1.

Table 1. Load vs. extension values of fabricated nanocomposites.

Sample-code	S 0	S 1	S 2	S 3	S 4	S 5
Load (N)	1963.3	2242.1	2494.5	3075.6	2439	2145.4
Extension (mm)	2.75	3.93	4.10	5.93	6.47	6.18

According to results, it is confirmed that a significant increase was observed in the tensile properties, Izod-impact and flexural strength and also in hardness for all series of HNTs addition (Table 1). Results for tensile strength depict that an increase of about 55.4% for sample X3 (already coded in Table 2 withrespect to unmodified specimen X0 (shown in Figure 3(a)–(b)). This shows an approximation for a reduction in pore size within the composite because of nanosized particles of HNTs and additionally confirmed by the increase in density of the composite which is an obvious and significant phenomenon (shown in Figure 3(c)) [24–26]

A similar effect for impact strength has been observed similarly as for flexural strength; however, an incredible increase in impact property has been found which increases 110.5% with respect to unmodified (X0) specimen (shown in Figure 3(d)). This might be due to the orientation of HNTs, process conditions and a partial diffusion of HNTs within the polymer epoxy resin [27]. An established is strain condition for the nanofiller (HNTs) and epoxy polymer generates an interfacial interaction that additionally depends on the dispersion of these Nano particulates with a successive increase in incorporation of nanosized grains within the base polymer matrix. Further, it is well adopted that this processing phenomenon increases by the amalgamation rate of the nano-size elements and a reduction of rejected particles from the matrix. Furthermore, due to this stress transfer increment, that additionally depends on the absorption and elastic range of the matrix. Here, for HNT/x (X = 3 wt.%), there is a reduction for slippage in polymer interface, and this might be the main cause for the mechanical property enhancement for fabricated HNT/Epoxy composite.

Table 2. Samples designation and formulations.

Sample code	Description	Experimental density (g/cm^3)		
		Test value range		Mean value (with deviation)
		Min value	Max value	
S 0	Cured unmodified	1.122	1.128	1.124 ± 0.004
S 1	Cured 1 wt.% HNT	1.158	1.176	1.162 ± 0.004
S 2	Cured 2 wt.% HNT	1.184	1.219	1.197 ± 0.022
S 3	Cured 3 wt.% HNT	1.203	1.246	1.236 ± 0.030
S 4	Cured 4 wt.% HNT	1.246	1.242	1.249 ± 0.005
S 5	Cured 5 wt.% HNT	1.246	1.285	1.273 ± 0.029

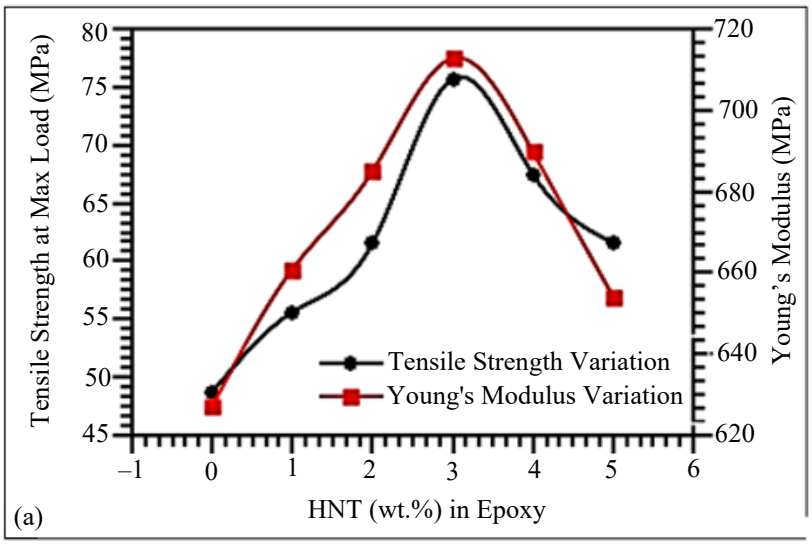

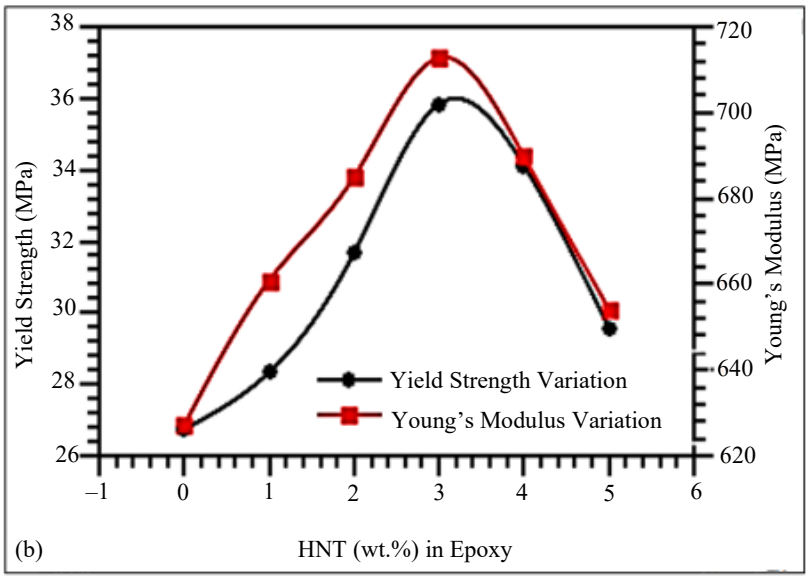

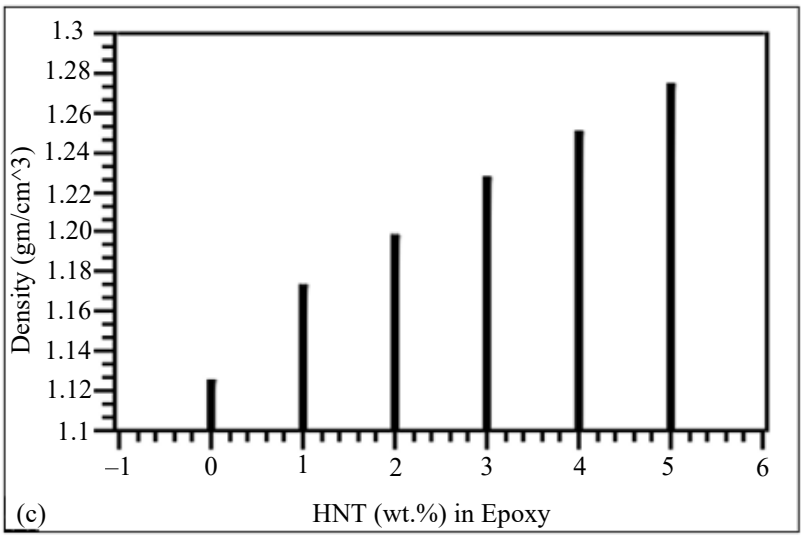

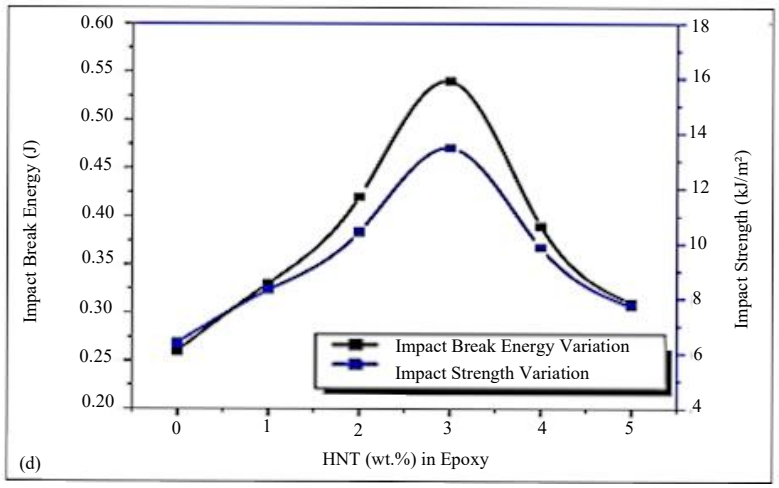

Figure 3. (a) Yield's strength and ultimate strength variation w.r.t. HNT wt.%, (b) yield's elongation in percentage and young's modulus changes with. HNT wt.%, (c) density changes with HNT/epoxy composite, and (d) impact break energy and strength as function of HNT/epoxy composite.

The enhanced properties mechanical in nature of modified nanocomposites associated with the unmodified cured epoxy matrix can be credited to the efficient transmission of stress from the epoxy matrix to HNT fillers. This stress transfer is mainly affected by the interfacial bonding amid the matrix and nanofiller, which depends on the dispersion and the bond of halloysite nanoparticles within epoxy matrix. It is well known that excessive strain can decrease stress transfer efficiency due to interfacial slippage between the filler and polymer matrix [28]. At an optimum HNT loading of 3 wt.%, the incorporation of nanotubular halloysite reduces interfacial slippage and improves stress transfer efficiency, leading to enhanced mechanical performance of the epoxy nanocomposites. The increase in Young's modulus and tensile strength with HNT addition is consistent with previously reported studies [29, 30]. This improvement can be accredited to the reinforcing effect of HNT fillers, that restrict polymer chain movement and enhance the stiffness of the epoxy matrix. Overall, the results support the rule of mixtures, which suggests that the incorporation of micro- and nanoscale reinforcements can effectively recover the mechanical performance of polymer composites compared with the neat epoxy matrix.

Table 1 highlights that the impact-strength properties of nanocomposite additionally improve with an increase of HNT's loading within the polymer epoxy matrix. Intrinsic toughening property of HNTs is responsible for improvement of impact strength, similarly as impact break energy and because of the presence of HNT's, tough and strong materials have been fabricated [31]. During deformation, impact strength, similarly as absorption break energy, has been enhanced because of better interfacial interaction. Here, proper distribution and good dispersion of nanotubular halloysite in a polymer epoxy matrix is responsible for high impact strength for developed nanocomposites [31, 32].

The high aspect ratio of HNTs compared with other reinforcement materials facilitates plastic deformation of the epoxy matrix and promotes complex matrix–filler interactions during nanotube fracture, pull-out, and bridging processes. As shown in Table 1, the improved hardness of the HNT/epoxy nanocomposites can be attributed to the incorporation of HNT particles, which increases the cross-linking density of the composite structure (Figure 4(a)) [33, 34].

The incorporation of 3 wt.% HNT (HNT/x, x = 3 wt.%) resulted in enhanced flexural-modulus and 34.8% rise in flexural strength compared with the unmodified epoxy matrix. However, further increases in HNT loading (4 and 5 wt.%) led to a reduction in flexural properties, which can be attributed to excessive nanotube content causing agglomeration and non-uniform dispersion of HNT particles within the epoxy matrix, as observed in Figure 4(b) and (c) [35].

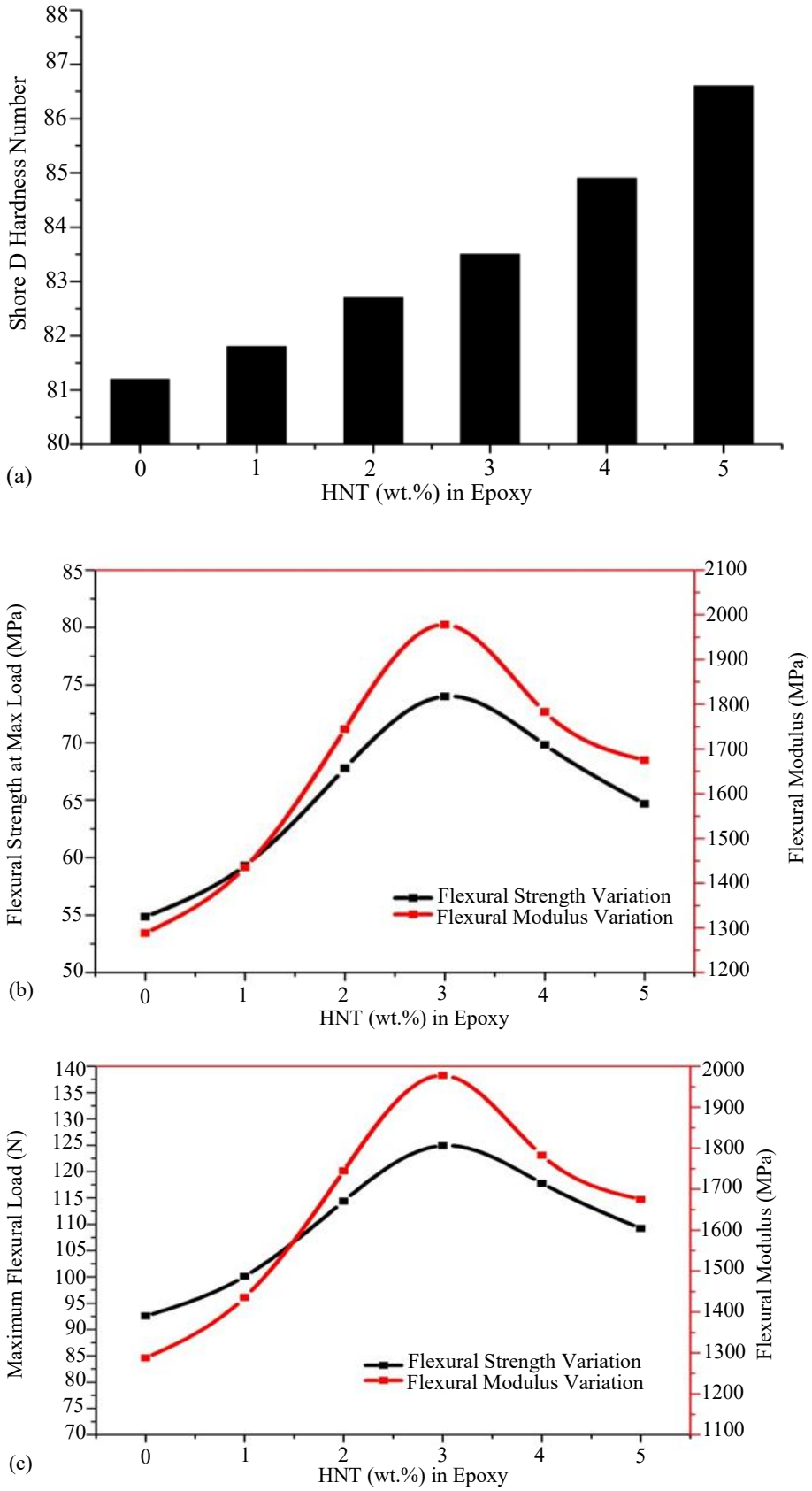

Figure 4. (a) Hardness variation w. r. t. HNT/epoxy composite, (b) flexural strength at max load and flexural modulus variation w.r.t. HNT wt.%, and (c) max flexural load and flexural modulus variation w.r.t. HNT wt.%.

Thermal Properties

TGA (Thermogravimetric Analyzer) Decomposition of unmodified epoxy takes place at 101°, whereas, for nanocomposites, the decomposition takes place at 122, 125, 132, 131 and 112° for varied loadings of HNT/x (x = 1 to 5 wt.%), respectively, as demonstrated in Table 1 and Figure 5 (a)–(f). Stability of epoxy matrix up to 132° could be explained from the crosslinking between the free hydroxyl groups [36], which might be present in the fatty acids or generated during the amine crosslinking reaction, in addition, as good chemical interactions via hydrogen bonding and polar–polar interactions. TGA thermograms clearly indicate that there is a significant enhancement in the thermal stability of developed HNT/Epoxy composites. The enhanced onset degradation temperature, reaching up to 310°C, can be accredited to the improved inter–facial interaction amid HNTs and the epoxy matrix, along with the effective bridging effect of the nanotubular fillers.

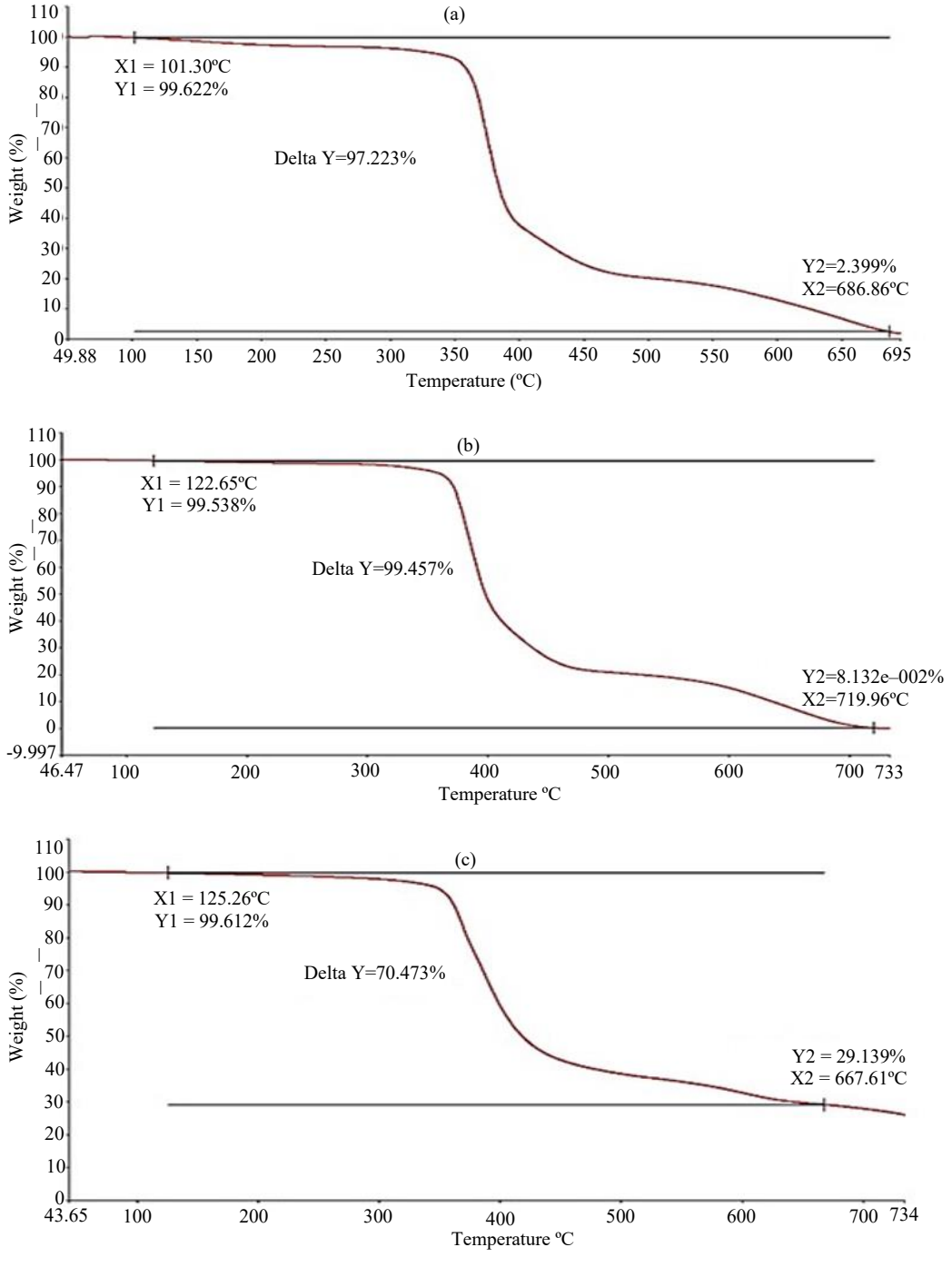

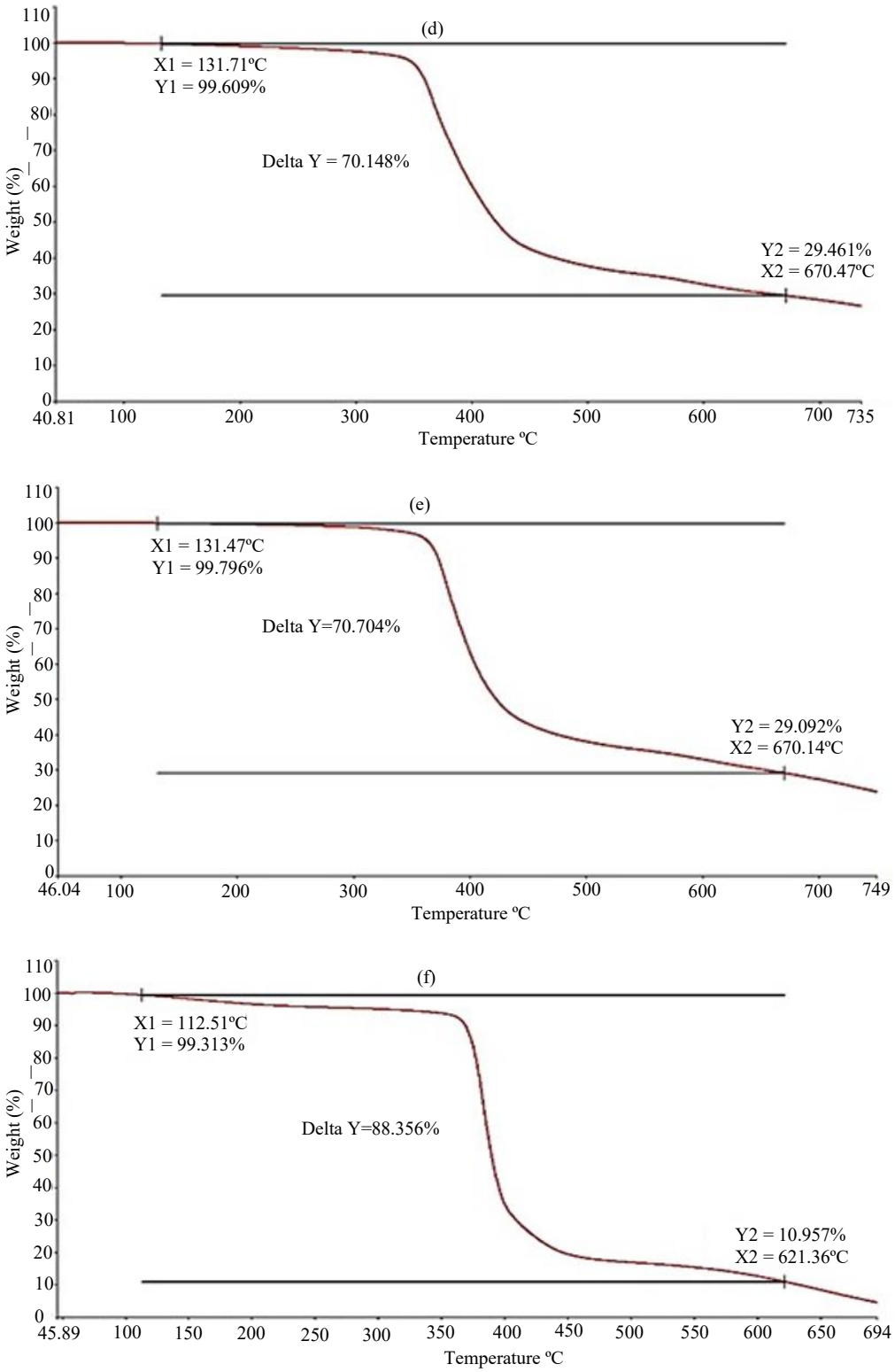

Figure 5. TGA thermograms of epoxy composites reinforced with different concentrations of halloysite nanotubes (HNTs): (a) unmodified epoxy, (b–f) HNT/epoxy composites containing 1, 2, 3, 4, and 5 wt.% HNT, respectively.

The increase in decomposition temperature of the modified nanocomposites can be primarily attributed to the confinement of polymer chains within the nanotube layers. The restricted movement of these polymer chains due to the layered structure of HNTs reduces segmental mobility, thereby

enhancing the thermal stability of the nanocomposites compared with the unmodified epoxy system. Furthermore, the formation of a protective char layer during thermal degradation may also contribute to the improved thermal resistance of the composites [37].

In the present investigation, overheating during ultrasonication was not actively controlled, yet premature curing was avoided by introducing the curing agent only after the sonication stage. However, no degradation or detriment in final composite qualities was detected even if a progressive increase in temperature was seen. However, the lack of a temperature control mechanism is a constraint, and future works should include regulated cooling (i.e., ice bath or pulsed sonication) to avoid probable nanotube damage or thermal deterioration.

Ultrasonic dispersion can improve epoxy wetting behavior and increase the surface area by shattering the agglomerates of HNT, thereby boosting the interfacial bonding at the molecular scale. This enhances the physicochemical interactions including hydrogen bonding and polar interactions between HNT surfaces and epoxy chains, which will result in better stress transmission and less interfacial defects in the composite system.

Morphological Studies by Scanning Electron Microscopy

Microstructural images (tensile fractured surface) for all composites (modified and unmodified) are clearly shown in Figure 6(a)–(f) for HNT/x (x = 0 to 5 wt. %). From these images, it is clear that the formation of shear bends and cracking of fibers for the fractured surfaces are variable according to the percentage of HNT's addition [38].

From Figure 6(a), in absence of HNTs, fracture damage is more and there is negligible amount of shear bend formation with respect to Figure 6(b)–(f). This confirms that sufficient ductility for modified composites appears whereas damaged fractured fiber appears in Figure 6(a). Closure microstructure for 3 wt. % HNT's addition confirms the uniform distribution of ductile wrinkles also with numerous shear particles for sizes less than 20 μm (Figure 6(d)). It is clearly found that cracked particles of HNT's stick on the composites' surfaces close to the wrinkles. Figure 6(e)–(f) confirm the variation of HNT's addition for tensile properties with numerous particles of HNTs (white phases) conjugated together, which are well stuck on the surfaces [12, 39].

From Figure 7(a), dimples as well as cracks have been observed also with particle overlapping (brittle asperities). The red box is used for the dimples and arrows are used for the crack formation. Effect of reinforcement addition on the nanocomposite can be found from Figure 7(b)–(f). Figure 7(b) (1 wt. % HNT addition) depicts numerous dimples and hollow cracks with crack blunting marked by red boxes and red circles. It is clear that some amount HNTs (white phase particles) are conjugated on hollow pores generated by tensile fracture of the matrix (shown by red circles) [40].

A huge amount of reinforcement deformation on the fractured surfaces appears which confirms the increase in shear stress distribution along the lateral surfaces. A particle distribution rate increases the surface energy distribution along the grain boundary and this distribution cracks when strain energy reaches to the surface energy. This also confirms the rate of ductility due to which tensile strain (elongation) increases; and was found maximum for 3 wt. % HNT and confirms the result that very less number of cracks and hollow blunt out appears [41].

In Figure 7(c), small size (less than 10 μm) and small fractured HNT's debris appear but on larger than 3 wt. % addition. A similar type of effect has been found in Figure 7(e)–(f); however, reinforcement cracking is less. Thus, it can be confined that with an increase in reinforcement amount, initially cracking of HNTs particles increases (maximum for 3 wt. %) and then decreases and can be seen in Figure 7(e)–(f).

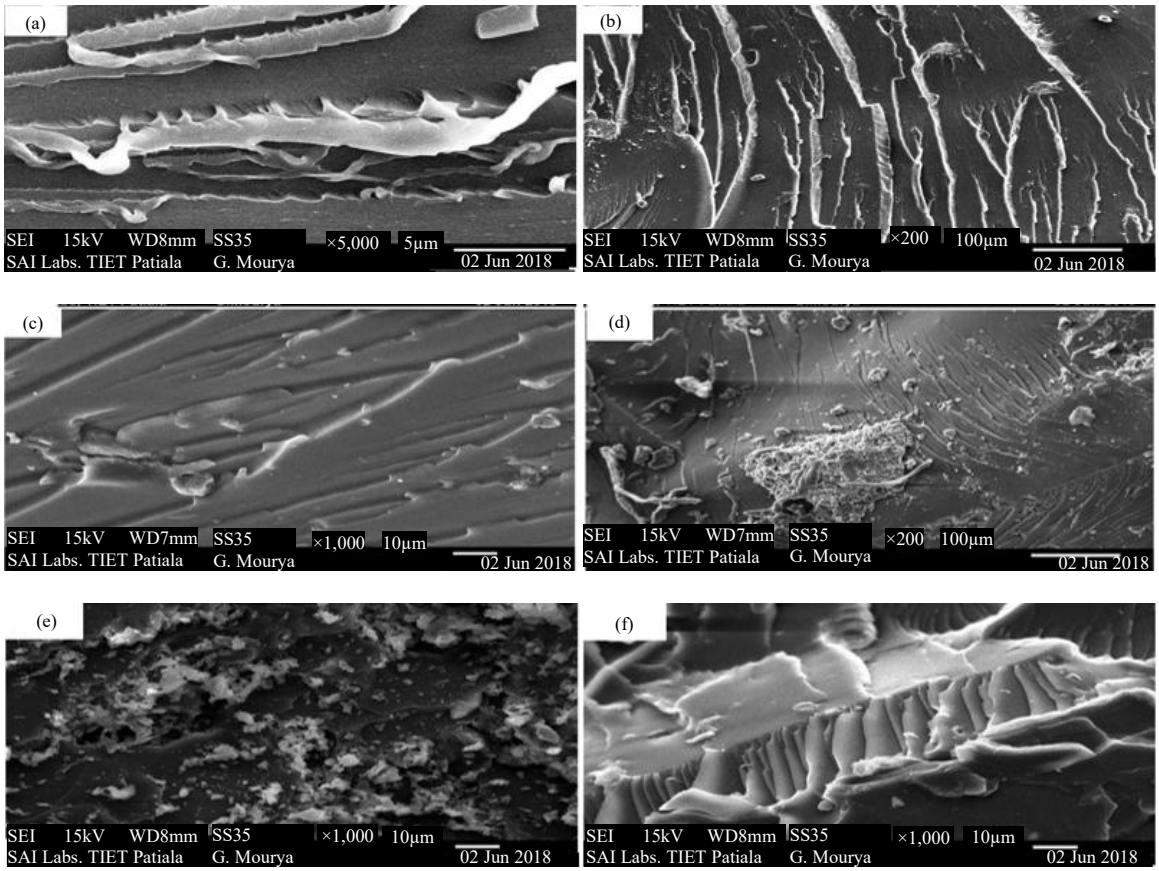

Figure 6. HNT/x/epoxy composites SEM images at: (a) x = 0 wt.%, (b) x = 1 wt.%, fractured fiber for HNT bunch, (c) x = 2 wt.%, interfaces and epoxy with wrinkles, (d) x = 3 wt.%, distributed bunches of the HNT, (e) x = 4 wt.%, closer observation for the HNT grains on the fractured surface, and (f) x = 5 wt.%, shear band formation and particle distribution.

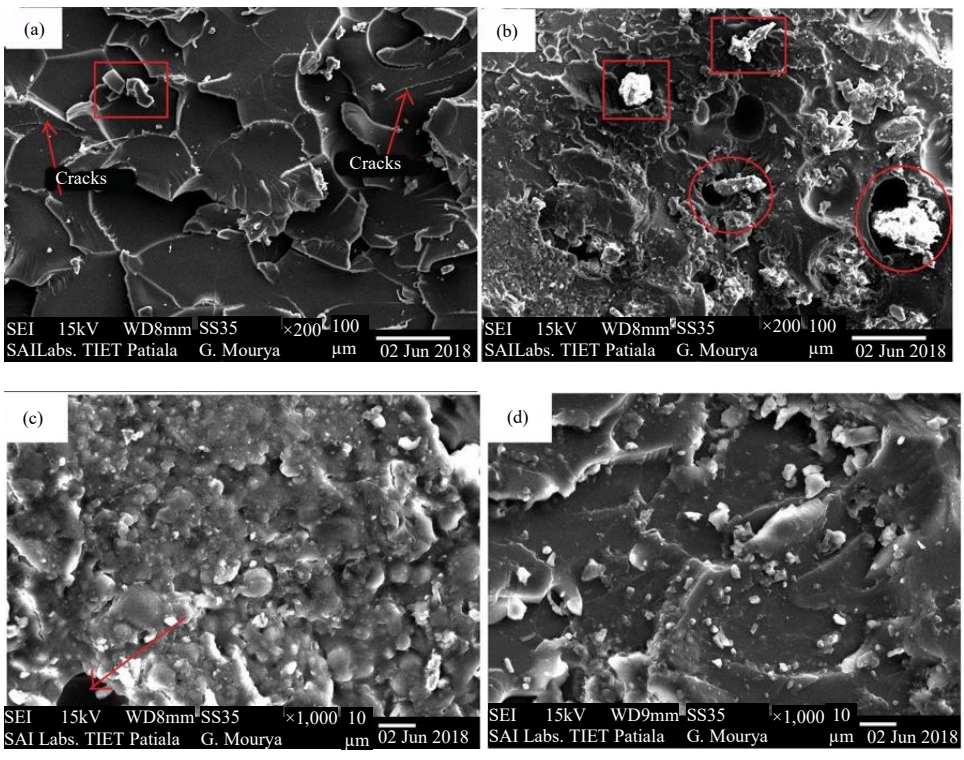

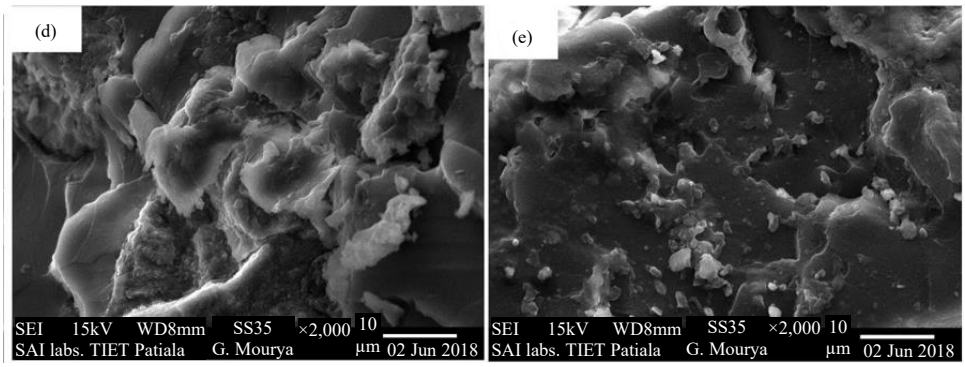

Figure 7. Micrograph for HNT/x/epoxy composites: (a) and (b) x = 1 wt.%, cracks and dimple on the fractured surfaces, (c) x = 2 wt.%, HNT particle cracking with epoxy, (d) x = 3 wt.%, distributed HNT particles on fractured surface, (e) x = 4 wt.%, fine dimples of the fractured surface, and (f) x = 5 wt.%, conjugated HNT particles on the fractured surface.

CONCLUSIONS

- Mechanical, thermal and microstructural evaluation of epoxy based HNTs reinforced nanocomposite, fabricated by casting method, for use in automobile and different environmentally safe applications, was carried out and following observations have been obtained:
  - The tensile strength of nanocomposite at maximum load has been increased by 55.4% after addition of 3 wt. % HNT, meanwhile, Young's modulus increased by 13.67% due to the constrained plastic deformation and load transfer between halloysite nanotube and epoxy resin. Although for all HNT/x (x=1 to 5 wt. %), tensile properties significantly improved when compared to unmodified epoxy.
  - Impact strength has been increased substantially for HNT/x (x = 3wt. %) nanocomposite which is about 110.5% as compared to the unmodified nanocomposite. Meanwhile, a similar trend was showed by HNT's addition on nanocomposites positively.
  - The improvements of 34.79 and 2.8% in flexural strength and shore D hardness were obtained upon addition of 3 wt. % Nanotubular halloysite, respectively, to the nanocomposite matrix.
  - Enhancement in the heat stability of the fabricated nanocomposite is clearly demonstrated by TGA. Due to halloysite nanotube bridging in modified composite with the epoxy resin, the onset temperature has been increased by 30.7%.
  - Microstructure examination depicts the influence of the insertion of reinforcement in the nanocomposite, accordingly, numerous dimples and hollow cracks with crack blunting are observed. Whereas some HNT particles conjugated on hollow pores, formed during the tensile test for the fractured matrix. Lateral surface microstructural images confirm the huge amount of reinforcement deformation and indicate an increase in shear stress distribution along the lateral surfaces.

REFERENCES

1. Yuan P, Tan D, Annabi-Bergaya F. Properties and applications of halloysite nanotubes: Recent Research Advances and Future Prospects. Appl Clay Sci. 2015;112–113:75–93.
2. Du M, Guo B, Jia D. Newly emerging applications of halloysite nanotubes: A Review. Polym Int. 2010;59(5):574–582.
3. Rao S, Thomas J, Aziz A, Cantwell W. Manufacturing and performance evaluation of carbon fiber–reinforced honeycombs. J Compos Sci. 2019 Jan 29;3(1):13.
4. Pasbakhsh P, De Silva R, Vahedi V, Churchman GJ. Halloysite nanotubes: Prospects and challenges of their use as additives and carriers–A Focused Review. Clay Miner. 2016 Jun;51(3):479–87.
5. Hanif M, Jabbar F, Sharif S, Abbas G, Farooq A, Aziz M. Halloysite nanotubes as a new drug-delivery system: A Review. Clay Miner. 2016 Jun;51(3):469–77.
6. Tang Y, Ye L, Deng S, Yang C, Yuan W. Influences of processing methods and chemical treatments on fracture toughness of halloysite–epoxy composites. Mater Des. 2012 Dec 1;42:471–7.
7. Ayatollahi MR, Shadlou S, Shokrieh MM. Fracture toughness of epoxy/multi-walled carbon nanotube nanocomposites under bending and shear loading conditions. Mater Des. 2011;32(4):2115–2124.

8. Chhetri S, Samanta P, Murmu NC, Kuila T. Anticorrosion properties of epoxy composite coating reinforced by molybdate-intercalated functionalized layered double hydroxide. J Compos Sci. 2019 Jan 15;3(1):11.
9. Azeez AA, Rhee KY, Park SJ, Hui D. Epoxy clay nanocomposites–processing, properties and applications: A Review. Compos Part B Eng. 2013 Feb 1;45(1):308–20.
10. Ragosta G, Abbate M, Musto P, Scarinzi G, Mascia L. Epoxy-silica particulate nanocomposites: Chemical interactions, reinforcement and fracture toughness. Polymer. 2005 Nov 14;46(23):10506–16.
11. Shadlou S, Ahmadi-Moghadam B, Taheri F. The effect of strain-rate on the tensile and compressive behavior of graphene reinforced epoxy/nanocomposites. Mater Des. 2014 Jul 1;59:439–47.
12. Ye Y, Chen H, Wu J, Ye L. High impact strength epoxy nanocomposites with natural nanotubes. Polymer. 2007 Oct 5;48(21):6426–33.
13. Köhler AR, Som C, Helland A, Gottschalk F. Studying the potential release of carbon nanotubes throughout the application life cycle. J Clean Prod. 2008 May 1;16(8–9):927–37.
14. Zeng QH, Yu AB, Lu GQ, Paul DR. Clay-based polymer nanocomposites: Research and commercial development. J Nanosci Nanotechnol. 2005 Oct 1;5(10):1574–92.
15. Joussein E, Petit S, Churchman J, Theng B, Righi D, Delvaux BJ. Halloysite clay minerals–A Review. Clay Miner. 2005 Dec 1;40(4):383–426.
16. Gamini S, Vasu V, Bose S. Tube-like natural halloysite/poly(tetrafluoroethylene) nanocomposites: Simultaneous Enhancement in thermal and mechanical properties. Mater Res Express. 2017;4 (4):045301.
17. Yu S, Tong MN, Critchlow G. Use of carbon nanotubes reinforced epoxy as adhesives to join aluminum plates. Mater Des. 2010;31(Suppl 1):126–129.
18. Palanisamy S, Murugesan TM, Palaniappan M, Santulli C, Ayrilmis N. Use of hemp waste for the development of mycelium-grown matrix biocomposites: A Concise Bibliographic Review. BioResources. 2023;18(4):8771–8780.
19. Ravichandran G, Ramasamy K, Manickaraj K, Kalidas S, Jayamani M, Mausam K, et al. Effect of sal wood and babool sawdust fillers on the mechanical properties of snake grass fiber-reinforced polyester composites. BioResources. 2025;20(4):8674–8694.
20. Kar A, Saikia D, Palanisamy S, Pandiarajan N. Effect of fiber loading on the mechanical, morphological, and dynamic mechanical characteristics of Calamus tenuis fiber reinforced epoxy composites. J Vinyl Addit Technol. 2025;31(1):224–240.
21. Pandiarajan P, Baskaran PG, Palanisamy S, Karuppusamy M, Marimuthu K, Rajan A, et al. Enhancing polyester composites with nano Aristida hystrix fibers: Mechanical and microstructural insights. BioResources. 2025;20(4):9257–9281.
22. Karuppusamy M, Kalidas S, Palanisamy S, Nataraj K, Nandagopal RK, Natarajan R, et al. Real-time monitoring in polymer composites: Internet of Things integration for enhanced performance and sustainability–A Review. BioResources. 2025;20(3):8093–8118.
23. Govindarajan PR, Shanmugavel R, Subramanian K, Palanisamy S, Santulli C, Fragassa C. Effect of stacking sequence on mechanical and water absorption characteristics of jute/banana/basalt fabric aluminium fibre laminates with diamond microexpanded mesh. Int J Polym Sci. 2024;2024(1):3835788.
24. Saif MJ, Asif M, Naveed M, Zia KM, Khosa MK, Jamal MA. Halloysite reinforced epoxy composites with improved mechanical properties. Green Sci. 2016 Mar 1;18(1):133–5.
25. Sun P, Liu G, Lv D, Dong X, Wu J, Wang D. Simultaneous improvement in strength, toughness, and thermal stability of epoxy/halloysite nanotubes composites by interfacial modification. J Appl Polym Sci. 2016 Apr 5;133(13).
26. Kumar S, Raju S, Mohana N. Effects of nanomaterials on polymer composites–An Expatriate View. Rev Adv Mater Sci. 2014 Sep 1;38(1):40.
27. Ye Y, Chen H, Wu J, Ye L. High impact strength epoxy nanocomposites with natural nanotubes. Polymer. 2007 Oct 5;48(21):6426–33.
28. Mu M, Osswald S, Gogotsi Y, Winey KI. An in situ Raman spectroscopy study of stress transfer between carbon nanotubes and polymer. Nanotechnology. 2009 Aug 19;20(33):335703.
29. Ngo TD, Ton - That MT, Hoa SV, Cole KC. Curing kinetics and mechanical properties of epoxy nanocomposites based on different organoclays. Polym Eng Sci. 2007 May;47(5):649–61.

30. Fu SY, Feng XQ, Lauke B, Mai YW. Effects of particle size, particle/matrix interface adhesion and particle loading on mechanical properties of particulate–polymer composites. Compos Part B Eng. 2008 Sep 1;39(6):933–61.
31. Deng S, Zhang J, Ye L, Wu J. Toughening epoxies with halloysite nanotubes. Polymer. 2008 Oct 30;49(23):5119–27.
32. Liu M, Guo B, Du M, Cai X, Jia D. Properties of halloysite nanotube–epoxy resin hybrids and the interfacial reactions in the systems. Nanotechnology. 2007 Nov 14;18(45):455703.
33. Lam CK, Cheung HY, Lau KT, Zhou LM, Ho MW, Hui D. Cluster size effect in hardness of nanoclay/epoxy composites. Compos Part B Eng. 2005 Apr 1;36(3):263–9.
34. Garcia C, Trendafilova I, Zucchelli A. The effect of polycaprolactone nanofibers on the dynamic and impact behavior of glass fibre reinforced polymer composites. J Compos Sci. 2018;2(3):43.
35. Kim MI, Kim S, Kim T, Lee DK, Seo B, Lim CS. Mechanical and thermal properties of epoxy composites containing zirconium oxide impregnated halloysite nanotubes. Coatings. 2017 Dec 15;7(12):231.
36. Han W, Yu Y, Tang Y, Sammut K. Nano-Halloysite Concentration Effects on Fracture Toughness of Diverse Epoxy Nanocomposites. Mater Perform Charact. 2014 Nov 1;3(3):506–18.
37. Park JH, Lee HM, Chin IJ, Choi HJ, Kim HK, Kang WG. Intercalated polypropylene/clay nanocomposite and its physical characteristics. J Phys Chem Solids. 2008 May 1;69(5–6):1375–8.
38. Vahedi V, Pasbakhsh P, Chai SP. Toward high performance epoxy/halloysite nanocomposites: New Insights based on rheological, curing, and impact properties. Mater Des. 2015 Mar 5;68:42–53.
39. Luo Z, Song H, Feng X, Run M, Cui H, Wu L, Gao J, Wang Z. Liquid crystalline phase behavior and sol–gel transition in aqueous halloysite nanotube dispersions. Langmuir. 2013 Oct 8;29(40):12358–66.
40. Tang Y, Deng S, Ye L, Yang C, Yuan Q, Zhang J, Zhao C. Effects of unfolded and intercalated halloysites on mechanical properties of halloysite–epoxy nanocomposites. Compos Part A Appl Sci Manuf. 2011 Apr 1;42(4):345–54.
41. Zeng S, Reyes C, Liu J, Rodgers PA, Wentworth SH, Sun L. Facile hydroxylation of halloysite nanotubes for epoxy nanocomposite applications. Polymer. 2014 Dec 1;55(25):6519–28.

